

# The Impact of Transmission Line Modeling on Lightning Performance of Line Surge Arresters - Part I: Impact on the Overvoltages<sup>\*</sup>

Jaimis S. L. Colqui<sup>\*</sup> Rodolfo A. R. Moura<sup>\*\*</sup>  
Marco Aurélio O. Schroeder<sup>\*\*</sup> José Pissolato Filho<sup>\*</sup>

<sup>\*</sup> School of Electrical and Computer Engineering, State University of  
Campinas, Brazil (e-mail: jaimis@unicamp.br; pisso@unicamp.br)

<sup>\*\*</sup> Electrical Engineering Department, Federal University of São João  
del-Rei, Brazil (e-mail: moura@ufsj.edu.br; schroeder@ufsj.edu.br)

---

**Abstract:** This paper investigates the influence of considering the performance of different calculation of transmission line parameters on the lightning performance of line surge arresters. The lightning performance of a surge arrester installed in a typical Brazilian 138-kV transmission line is assessed, while transmission line parameters are calculated in 3 different ways namely: i) Carson formulation, ii) Nakagawa formulation considering the electrical parameters of the ground constant with the frequency, and iii) Nakagawa formulation considering the frequency-dependent characteristics of soil. Taking as reference the results determined using the Carson formulation, it is shown that the Nakagawa formulation constant and dependent with the frequency can lead to possible incorrect prevision of insulation failure in lines partially protected by lightning surge arresters. According to the results, depending on the case, maximum differences of 6.01% and 6.42% can be found, respectively.

*Keywords:* Transmission line modeling; surge arresters; lightning protection; frequency dependent behaviour; grounding; time-domain simulations.

---

## 1. INTRODUCTION

Lightning-related phenomena are the main causes of transmission lines (TL) shutdowns (De Castro et al., 2017). In TLs studies, differently from distribution lines, only the direct incidences are capable of interrupting the line (Paulino and Fonseca, 2019). Moreover, TL are usually designed to shield the incidence in phase cables by allocating shield wires above the TL. In these cases, the most widely used practice to improve the TL lightning performance is to reduce grounding impedance, which directly impacts on the reduction of resulting overvoltages in the insulator strings (Alipio et al., 2018).

Additionally, in the case of TLs in regions where the soils have high resistivity, achieving reduced values of grounding impedance is either technically or economically unfeasible. In these situations, it has been common practice to use surge arrester (SA) devices (Alipio et al., 2018; Visacro et al., 2020; Castro et al., 2022). These devices are installed in parallel with insulator strings. In this sense, the grounding system also plays a relevant role in the performance of the lightning arrester (Alipio et al., 2018).

The impact evaluation of installing SA for improving TL lightning performance, electromagnetic transients programs type (EMTP-type) in the time domain are usually used to carry out simulations, since non-linear devices, such as SA, are more correctly addressed in this domain.

---

<sup>\*</sup> This work was supported by São Paulo Research Foundation (FAPESP) (grant: 2021/06157-5).

However, these programs do not have, natively, appropriate models to represent the frequency response of grounding system neither the frequency-dependence behavior of the soil.

Even so, EMTP-type do not consider this behavior in the TL models, and in most of these programs they compute the ground effect using the classic Carson formulation, which assumes the conduction current in the ground is much higher than the displacement current and ignores the variation of the ground parameters with the frequency (Carson, 1926). These assumptions can lead to errors in the case of high resistivity soils and applications involving high frequencies, such as transients arising from the incidence of lightning in TLs (Diniz et al., 2022).

In recent works, the impact of considering SA in TLs were evaluated using a fullwave grounding model, but with regard to TL models, the calculation of parameters is still computed with the classical Carson formulation (Vasconcellos et al., 2022; Banjanin, 2018). Since lightning strikes have frequency components ranging from 0 Hz to a few MHz, this simplified formulation for calculating line parameters can lead to incorrect simulation results.

In this context, we intend to evaluate the impact of the of the simplified formulation of the calculation of the line parameters in computer simulations in the performance of SA devices. This work is divided into two parts. In Part I, the models used to simulate electromagnetic transients in TLs protected by SA are detailed. In this same part, the results are presented that illustrate the impact the

simplified formulation of the calculation of the line parameters on the resulting overvoltages in the insulator string of phases protected or not by SA. In Part II, results are presented that show the impact the simplified formulation of the calculation of the line parameters in the power and energy estimate absorbed by SA.

The paper is organized as follows: Section 2 presents the models used to simulate the electromagnetic transients in the software Alternative Transients Program (ATP). Section 3 is devoted to present the impact of the formulations of the calculation of TL parameters. The main conclusions of this paper are presented in Section 4.

## 2. SYSTEM DESCRIPTION

In order to assess the impact of transmission line modeling on the lightning arrester performance, it is considered a simple circuit 138-kV TL, typically found in Brazil (Schroeder et al., 2018). Fig. 1(a) shows the tower silhouette with their corresponding line cable heights. The transmission line has one conductor per phase, LINNET code, and a 3/8" EHS shield wire. The geometric coordinates of the phase conductors and shield wire are shown in Fig. 1(a).

In the simulations, eleven towers and twelve spans are considered where the incidence of lightning was at the top of the central tower. Five adjacent towers (identical to Fig. 1(a)) are included in the simulations to consider the propagation effects of overvoltage waves in the line conductors, as well as the reflections that occur in the adjacent spans. The spans between the central tower (where the incidence occurs) and the adjacent towers are 380-m long.

Fig. 1(b) shows the a typical grounding arrangement for this type of TL. It consists of 4 counterpoises cables with a radius of 7 mm, buried at a 0.5 m depth, each starting one foot from the base of the tower. The length L of the counterpoises cables is selected according to the soil resistivity value.

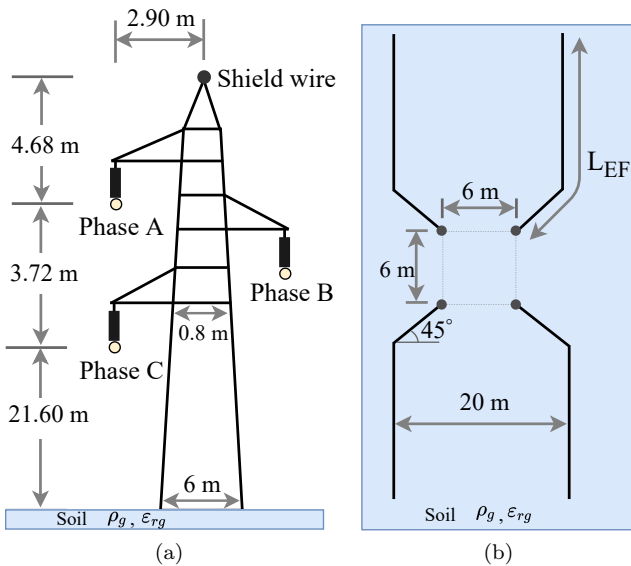


Figure 1. (a) Tower silhouette, and (b) Grounding arrangement.

The modeling of each component are briefly described hereafter.

### 2.1 Tower Model

The tower is modeled as a lossless single-phase TL, for which the surge impedance is calculated using the revised Jordan's formula, which was extended in De Conti et al. (2006) to take into account vertical multiconductor systems. Considering that the tower can be represented by  $n$  vertical conductors and that they are connected at the current injection point, it is possible to represent the whole multiconductor system as a single TL with equivalent surge impedance  $Z_{eq(i)}$  given by (De Conti et al., 2006)

$$Z_{eq(i)} = \frac{Z_{i1} + Z_{i2} + \dots + Z_{ii} + \dots + Z_{in}}{n} \quad (1)$$

where

$$Z_{ii} = 60 \ln \left( \frac{4h}{r} \right) - 60 \quad (2)$$

$$Z_{ij} = 60 \ln \frac{2h + \sqrt{4h^2 + d_{ij}^2}}{d_{ij}} + 30 \frac{d_{ij}}{h} - 60 \sqrt{1 + \frac{d_{ij}^2}{4h^2}} \quad (3)$$

where  $h$  is the height of the conductor,  $r$  is the conductor radius, and  $d_{ij}$  corresponds to the distance between the centers of conductor  $i$  and  $j$ .

In particular, the tower of Fig. 1(a) was divided into four sections, each one represented by four vertical conductors. The lower portion of the tower was represented as a cascade of three TLs (one 23.25-m and two 1.86-m), while its upper part was represented as a single 3.03-m long TL. The equivalent impedance of each tower segment was computed using (1), (2) and (3), considering average distances between tower conductors and assuming  $r=6.5$  cm.

### 2.2 Transmission Line Model

Two models are adopted in this paper to represent the TL. The first is the J. Marti model (Marti, 1982), which is available in the ATP software considers Carson's equations for calculating the Line parameters and a Bode's method for synthesize the characteristic impedance  $Z_c$  and propagation function  $H$  matrices (Prikler and Hoidalén, 2009). These implemented equations only consider the electrical parameters of the ground constant with the frequency and neglect the displacement currents in the calculation of the impedance and admittance of ground return.

In order to evaluate the effect of frequency dependent soil parameters and considered the displacement currents in the simulation of lightning overvoltages on TLs, a second model, here called modified Marti's model (De Conti and Emídio, 2016), implemented in ATP is used. The implementation of modified Marti's model employ the Vector Fitting method (Gustavsen and Semlyen, 1999) to fit the matrices  $Z_c$  and  $H$ .

The calculation of the series impedance and the transversal admittance of a line is given by (Diniz et al., 2022):

$$\mathbf{Z} = \mathbf{Z}_{int} + \frac{j\omega\mu_0}{2\pi} (\mathbf{M} + \mathbf{S}_1) \quad (4)$$

$$Y = j\omega\varepsilon_0 2\pi (\mathbf{M} + \mathbf{S}_2)^{-1} \quad (5)$$

where  $Z_{int}$  is the internal impedance of the conductor,  $\mathbf{M}$  is the term that relates the external fields in the air,  $\mathbf{S}_1$  and  $\mathbf{S}_2$  are the ground return impedance and admittance terms, respectively. In this work, the ground admittance was calculated considering the soil as a perfect electrical conductor ( $\mathbf{S}_2 = 0$ ), because the soil effect has a negligible in the admittance calculation in the frequency range of interest in this work (Alípio et al., 2019).

The difference between the Carson (Carson, 1926) and Nakagawa (Nakagawa, 1981) formulations is the approximation used for the term  $\mathbf{S}_1$ . While Carson determines the ground return impedance through (6), Nakagawa determines it through (7).

$$\mathbf{S}_{1(CA.)} = \int_0^\infty \frac{2e^{-2h\lambda}}{\lambda + \sqrt{\lambda^2 + j\omega\mu_0\sigma_g}} \cos(r\lambda) d\lambda \quad (6)$$

$$\mathbf{S}_{1(NA.)} = \int_0^\infty \frac{2e^{-2h\lambda}}{\lambda + \sqrt{j\omega\mu_0(\sigma_g + j\omega\varepsilon_0(\varepsilon_{rg} - 1))}} \cos(r\lambda) d\lambda \quad (7)$$

where  $\omega = 2\pi f$  is the angular frequency in [rad/s],  $\mu_0$  is the vacuum permeability in [H/m],  $\varepsilon_0$  is the vacuum permittivity in [F/m],  $\varepsilon_{rg}$  is the relative permittivity,  $\sigma_g$  is the soil conductivity in [S/m],  $r$  is the horizontal separation between conductors in [m],  $h$  is the heights of conductors above the soil in [m].

In the modified JMarti model of the TL, it is taking into account the frequency dependence of the electrical parameters of the soil, resistivity and permittivity. According to Colqui et al. (2021), such dependence can impact the behavior of the TL, especially in those cases where the TLs are installed in high resistivity media. Since SA are mainly installed on lines installed in regions of high resistivity, it is important to take this effect into account when calculating the transient overvoltage response.

In this work, the frequency dependence of the electrical parameters of the soil is considered based on the application of a causal physical model developed by Alípio-Visacro, based on a large number of field measurements Alípio and Visacro (2014). This model was recently recommended by CIGRE Working Group C4.33 (2019) for lightning-related studies. Equations (8) and (9) illustrate the formulation of the model.

$$\sigma_g(f) = \sigma_0 + \sigma_0 \times h(\sigma_0) \left( \frac{f}{1\text{MHz}} \right)^\xi \quad (8)$$

$$\varepsilon_{rg}(f) = \varepsilon_{r\infty} + \frac{\tan(\pi\xi/2) \times 10^{-3}}{2\pi\varepsilon_0(1\text{MHz})^\xi} \sigma_0 \times h(\sigma_0) f^{\xi-1} \quad (9)$$

where  $\sigma_0$  is the DC conductivity in [mS/m],  $\varepsilon_{r\infty}$  is the relative permittivity at higher frequencies, and  $f$  is the frequency in [Hz]. According to Alípio and Visacro (2014), the following parameters are recommended in (8) and (9) to obtain mean results for the frequency variation of  $\sigma_g$  and  $\varepsilon_{rg}$ :  $\xi = 0.54$ ,  $\varepsilon_{r\infty} = 12$  and  $h(\sigma_0) = 1.26 \times \sigma_0^{-0.73}$ .

### 2.3 Surge Arresters

The data from the surge arrester used to perform the simulations are from a commercial SA manufactured by

Siemens (Vasconcellos et al., 2022). This SA is considered suitable for protecting TLs of 138-kV against atmospheric surges. The main characteristics of this SA are summarized in Table 1. To represent this device in the simulations the model suggested by the IEEE (1992) is considered. The parameters of this model are obtained according to the procedure described in IEEE (1992), considering the data in Table 1.

Table 1. Surge Arrester Data.

Line discharge class	2
Height of the arrester (m)	1.24
Number of parallel columns of MO	1
Rated voltage (kV)	132
Continuous operating voltage (kV)	106
Residual voltage for a 1 kA 30/60 us current (kV)	269
Residual voltage for a 10 kA 8/20 us current (kV)	337

### 2.4 Insulator Strings

In this work, it has been adopted the Disruptive effect method (DE method) approach, since it is easy to obtain its parameters and it also presents an excellent accuracy (Hileman, 1999). The DE method concept is based on the idea of the existence of a critical disruptive effect  $DE_C$  for each insulator configuration. Each non-standard voltage surge has an associated disruptive effect (DE). If this DE value exceeds the critical value, a disruptive discharge occurs, which causes the insulation to break (Hileman, 1999). The disruptive effect associated with a voltage waveform is determined by

$$DE = \int_{t_0}^{t_a} (v(t) - V_0)^k dt \quad (10)$$

where  $v(t)$  corresponds to the voltage waveform applied over the insulator string,  $V_0$  refers to the voltage threshold from which it has begun the process of rupture in the insulator,  $t_0$  is the instantaneous value of  $v(t)$  exceeds  $V_0$ ,  $k$  is a dimensionless factor, and  $DE$  is the variable called "disruptive effect". For a typical 138-kV line, DE method constants can be obtained according to Hileman (1999):  $DE_c = 1.1506 (CFO)^k$ ;  $k = 1.36$ ;  $V_0 = 0.77 CFO = 500.5$  kV.

### 2.5 Tower-footing Grounding

The tower-footing grounding system plays a fundamental role in backflashover occurrence when the shield wire and the tower are subjected to direct strikes. To calculate the grounding impedance, was use the Hybrid Electromagnetic Model (HEM) with frequency dependent electrical parameters of the soil.

The impedance  $Z(\omega)$  of the tower-footing grounding is determined using the accurate HEM (Visacro and Soares, 2005), in a frequency range from DC to several MHz. As detailed Visacro and Soares (2005), the HEM solves Maxwell's equations numerically via the vector and scalar potentials using the thin wire approximations. In the calculations, the frequency dependence of the soil parameters is taken into account using (8) and (9). After determining the harmonic impedance  $Z(\omega)$ , a pole-residue model of the associated admittance  $Y(\omega) = 1/Z(\omega)$  is obtained using the vector fitting (VF) method (Gustavsen and Semlyen,

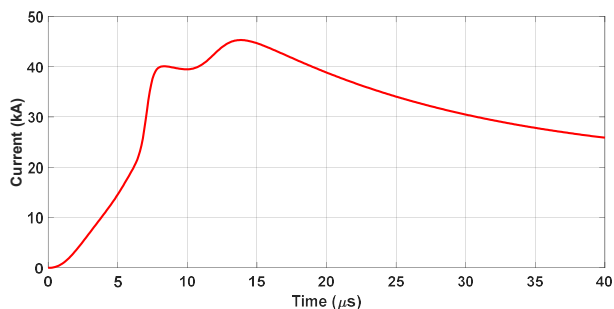


Figure 2. Representative lightning current waveform of first strokes measured at Morro do Cachimbo Station.

1999). Finally, an electrical network is synthesized from the passive pole residue model corresponding to the grounding admittance. Both the pole-residue model and the electrical network were obtained using the VF toolbox available to third parties from VF website (Gustavsen, 2022; Gustavsen and Semlyen, 1999).

### 2.6 Lightning Current

A proper evaluation of lightning effects on power systems relies upon, among other factors, on an appropriate representation of the lightning current waveform since the quality of the simulation results depends on the representativity of the assumed lightning current waves. According to (Visacro et al., 2004), the first stroke currents are characterized by a pronounced concavity at the front and by the occurrence of multiple peaks, being the second peak usually the highest one, and the maximum steepness occurring near the first peak according to measurements of instrumented towers, such as those presented in Visacro et al. (2004). Considering the previous aspects, the simulations were performed considering the main median parameters of first strokes measured at Morro do Cachimbo Station. As detailed in De Conti and Visacro (2007), the waveforms of Fig. 2 are obtained by a sum of Heidler functions and the current waveform depicted in Fig. 2.

## 3. RESULTS

This section presents simulation results of overvoltages developed along the insulator strings (phases A, B and C) of a 138-kV line due to the incidence of lightning at the top of the tower. All simulations were carried out with the ATP and the main objective is to evaluate the impact of the representation of the TL models on the performance of the surge arrester, an extensive set of simulations was carried out, contemplating partially protected lines (lightning arresters in one or in two phases) and fully protected (lightning arresters in all phases).

In order to compare the aforementioned models on TLs, Table 2 summarizes four different representations, deliberately chosen, of the transmission system models. These representations were set to be used in the simulations. Also, the low-frequency soil resistivities considered are: 1000, 3000 and 10000  $\Omega$ .m. For these resistivities, it was considered the effective length, obtained by using ref CIGRE Working Group C4.23 (2021). The effective length and low frequency resistance of the counterpoise cable are shown in Table 3.

Table 2. Types of modeling representations.

TL model	Appro.	Soil for TL	Ground. model
JMarti	Carson	$\rho_0$	$Z(\rho(\omega), \epsilon_r(\omega))$
Modified Marti's	Nakagawa	$\rho_0, \epsilon_r$	$Z(\rho(\omega), \epsilon_r(\omega))$
Modified Marti's	Nakagawa	$\rho(\omega), \epsilon_r(\omega)$	$Z(\rho(\omega), \epsilon_r(\omega))$

Table 3. Length of the counterpoise wires as a function of soil resistivity.

$\rho_0$ [ $\Omega$ .m]	1000	3000	10000
$L_{EF}$ [m]	55	100	180

Results of comparisons of overvoltages along the insulator strings are presented in the subsection 3.1, for a current wave with a median peak value according to measurements at the Morro do Cachimbo station. In the subsection 3.2, graphs of the percentage deviations of the comparisons of the TL models for the set of simulations shown in the subsection 3.1 are presented.

### 3.1 Overvoltages Across the Insulator String

Figs. 3, 4 and 5 illustrate the overvoltages across insulator strings of phases A, B and C of the 138-kV line, considering the various representations of the TL shown in Table 2, contemplating lines partially protected and completely protected, and the soil resistivities of 1000  $\Omega$ .m, 3000  $\Omega$ .m and 10000  $\Omega$ .m. In all figures it can be seen that the overvoltages developed in the insulator strings when contemplating lines without SA are greater for all phases than when contemplating SA in phase C, at the same time they are greater if contemplating SA in phases B and C, and these are greater if we contemplate SA in phases A, B, and C. Likewise, it can be noted that the overvoltages in all phases when we consider a soil with a resistivity of 1000  $\Omega$ .m, are smaller than the overvoltages when we consider a soil with a resistivity of 3000  $\Omega$ .m, and these are smaller than the overvoltages when we consider a soil with a resistivity of 10000  $\Omega$ .m.

In the case of Fig. 3, it can be observed that for all representations of the TL and SA no differences are observed in the wavefronts or along the tail. This is because for the resistivity of 1000  $\Omega$ .m the electrical parameters of the TL models do not have much difference (Colqui et al., 2021). In this range of the spectrum, the Carson and Nakagawa model with constant and frequency-dependent ground parameters are practically equivalent.

In the case of Fig. 4, it can be observed that, for some representations of the TL and SA, small differences in wavefronts can be found. This occurs because for the resistivity of 3000  $\Omega$ .m although the soil parameters can impact the TL model, it is not very sensitive to this influence. This can be even more noticeable along the tail since in the low frequency components (associated with the tail) the difference between the methods are practically nonexistent. In this range of the spectrum, the Carson and Nakagawa model with constant and frequency-dependent soil parameters begins to show very similar results. At the peaks of the overvoltages for the Carson and Nakagawa formulations with frequency-constant parameters they present maximum differences of 1.19%, and 1.01% in relation to Nakagawa Formulation considering

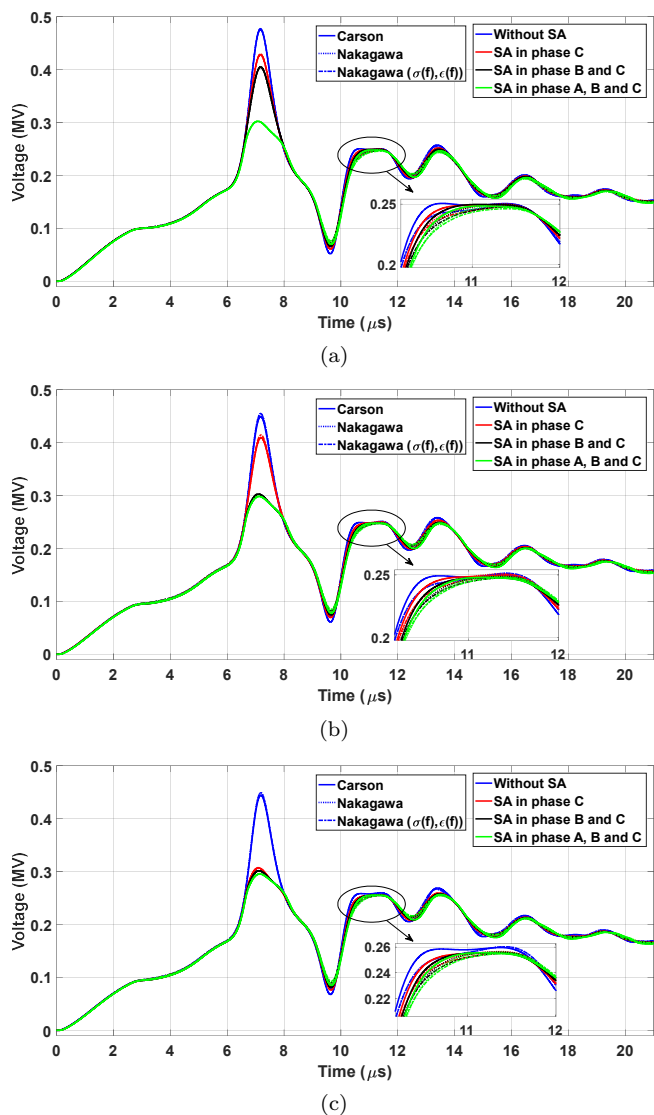


Figure 3. Overvoltages across the insulator string of the line, considering soil with  $\rho_0=1000 \Omega.m$ ; (a) Phase A, (b) Phase B and (c) Phase C.

the frequency dependence of the soil, which is the most complete representation addressed in this paper.

In the case of Fig. 5, it can be observed that for some representations of the TL and SA greater differences in waveform than the case of  $3000 \Omega.m$  and  $1000 \Omega.m$ . This is because for the resistivity of  $10,000 \Omega.m$  the electrical parameters of the TL models have a considerable difference at high frequencies (Colqui et al., 2021). However, similarly to the previous cases, along the tail no differences are observed. Also, at the peaks of the overvoltages for the Carson and Nakagawa formulations with frequency-constant parameters they present maximum differences of 2.90%, and 1.27% in relation to Nakagawa Formulation considering the frequency dependence of the soil.

As shown in this section, when using Carson and Nakagawa formulations with constant soil parameters to evaluate overvoltage calculations, for example, the results can be erroneous and therefore it is preferable to use a more ac-

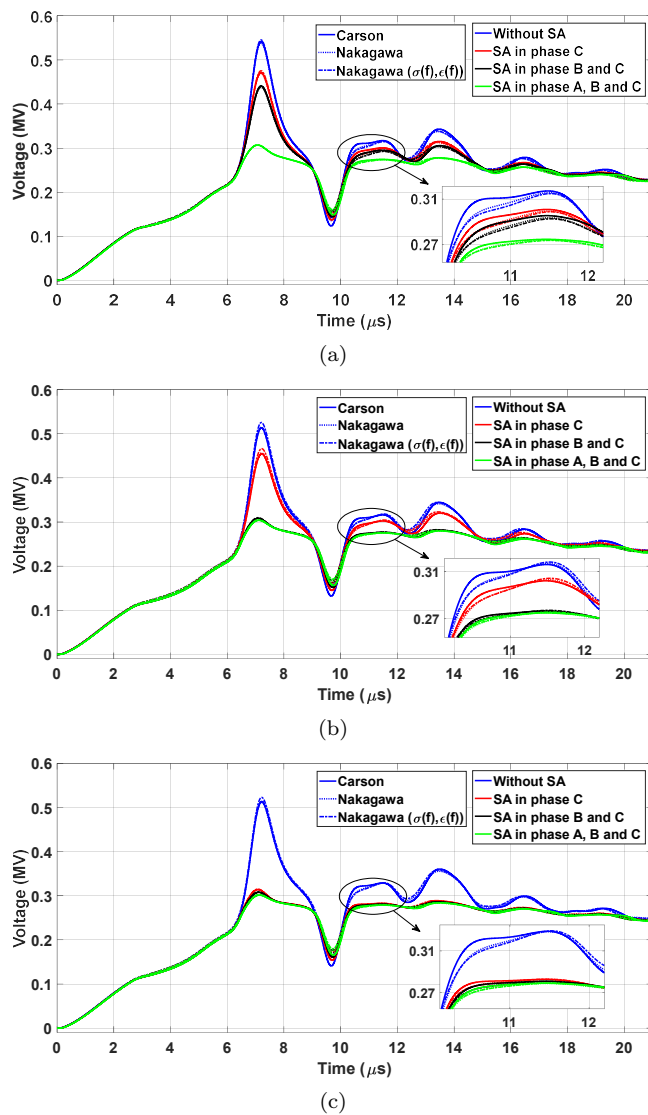


Figure 4. Overvoltages across the insulator string of the line, considering soil with  $\rho_0=3000 \Omega.m$ ; (a) Phase A, (b) Phase B and (c) Phase C.

curate formulation, which take into account the frequency dependence of the electrical parameters of the ground.

### 3.2 Percentage Deviations from Overvoltages Across the Insulator String

Figs. 6, 7 and 8 illustrate the percentage deviations from overvoltages (across insulator strings of phases A, B and C) shown in the Figs. 3, 4 and 5. All these comparisons correspond to the percentage deviation between the overvoltages calculated by the Nakagawa's formulation (NA) in relation to the Carson's formulation (CA). The percentage deviation ( $\Delta V(\%)$ ) is computed as follows

$$\Delta V(\%) = \frac{V_{CA} - V_{NA}}{V_{CA}} \times 100\% \quad (11)$$

For the three resistivities and for all comparisons, there are differences in percentage deviations when Carson and Nakagawa formulations are compared with Carson and Nakagawa formulations but considering frequency-dependent soil parameters. Likewise, it can be noted that the devia-

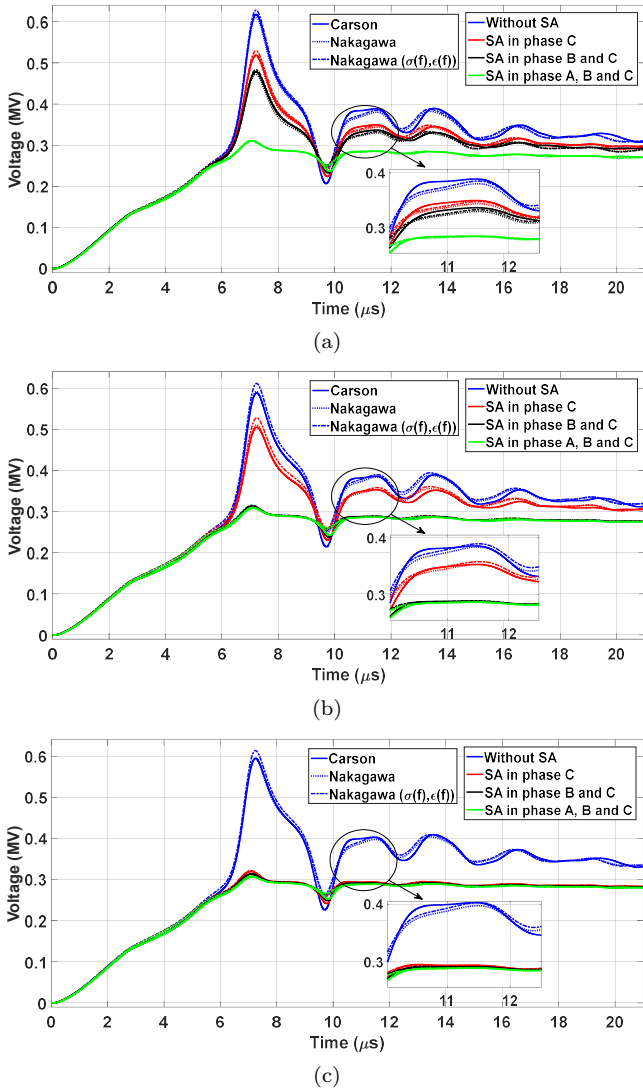


Figure 5. Overvoltages across the insulator string of the line, considering soil with  $\rho_0=10000 \Omega.m$ ; (a) Phase A, (b) Phase B and (c) Phase C.

tions in all phases when we consider a soil with a resistivity of  $1000 \Omega.m$ , are smaller than the deviations when we consider a soil with a resistivity of  $3000 \Omega.m$ , and these are smaller than the deviations when considering a soil with a resistivity of  $10000 \Omega.m$ .

In the case of Fig. 6, the maximum differences of the comparisons of the perceptual deviations between Carson and Nakagawa formulations are of 2.81%, 2.97%, and 2.96% for phases A, B and C. In the case of Fig. 7, the maximum differences of the comparisons of the perceptual deviations between Carson and Nakagawa formulations are of 5.02%, 5.56%, and 5.58% for phases A, B and C. In the case of Fig. 7, the maximum differences of the comparisons of the perceptual deviations between Carson and Nakagawa formulations are of 5.90%, 6.42%, and 6.18% for phases A, B and C.

The analysis considered different formulations of the calculation of transmission line parameters on the lightning performance of line surge arresters. As shown in this section, when using Carson and Nakagawa formulations

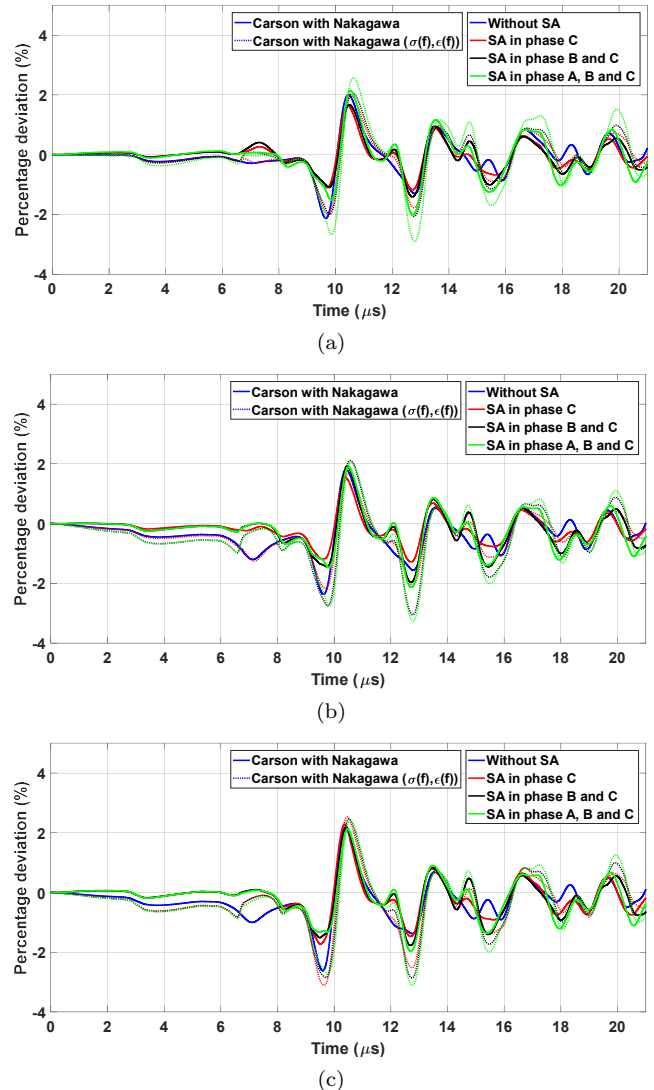


Figure 6. Percentage deviation of the Nakagawa formulation in relations with Carson formulation, considering soil with  $\rho_0=1000 \Omega.m$  the Fig. 3; (a) Phase A, (b) Phase B and (c) Phase C.

with constant soil parameters to evaluate the impact on the lightning arresters, for example, the results can be erroneous and therefore it is preferable to use more accurate Nakagawa formulations, which take into account the frequency dependence of the electrical parameters of the ground.

#### 4. CONCLUSIONS

In this work, the impact of the formulations for calculating the transmission line parameters on the TL lightning overvoltages performance was evaluated. Three representations for the line parameters were considered: i) Carson formulation, ii) Nakagawa formulation with ground parameters constant with frequency, and iii) Nakagawa formulation with ground parameters variable with frequency. From the simulation results, the following main conclusions were reached:

- Results show small differences in simulated lightning overvoltages assuming or neglecting the frequency de-

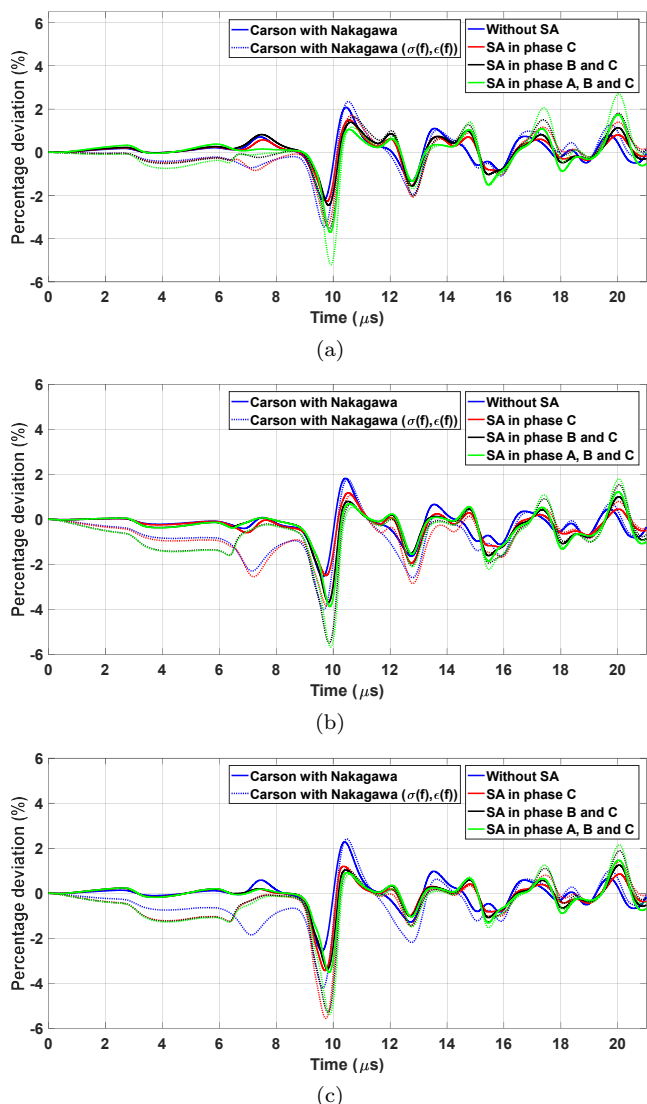


Figure 7. Percentage deviation of the Nakagawa formulation in relations with Carson formulation, considering soil with  $\rho_0=3000 \Omega.m$  in the Fig. 4; (a) Phase A, (b) Phase B and (c) Phase C.

pendence of soil parameters. These differences became larger with increasing the value of the soil resistivity and might be important in determining the probability of critical currents occurrence.

- In phases not protected by surge arresters, the Nakagawa formulations lead to small differences in overvoltage levels from those determined by adopting the Carson formulation. Although very conservative, the Carson's formulations could change the probabilities of failure occurrence incorrectly and higher values.
- In phases protected by surge arresters, very small differences are observed in the overvoltage waveforms, basically on the wavefront, considering the three formulations for calculating the line parameters. Apparently, the presence of the surge arrester tends to reduce the impact of the line formulation. Although such differences are not enough to imply a change in the performance of the surge arrester in preventing the occurrence of a break in the insulator strings, they can lead to incorrect estimates of the power and

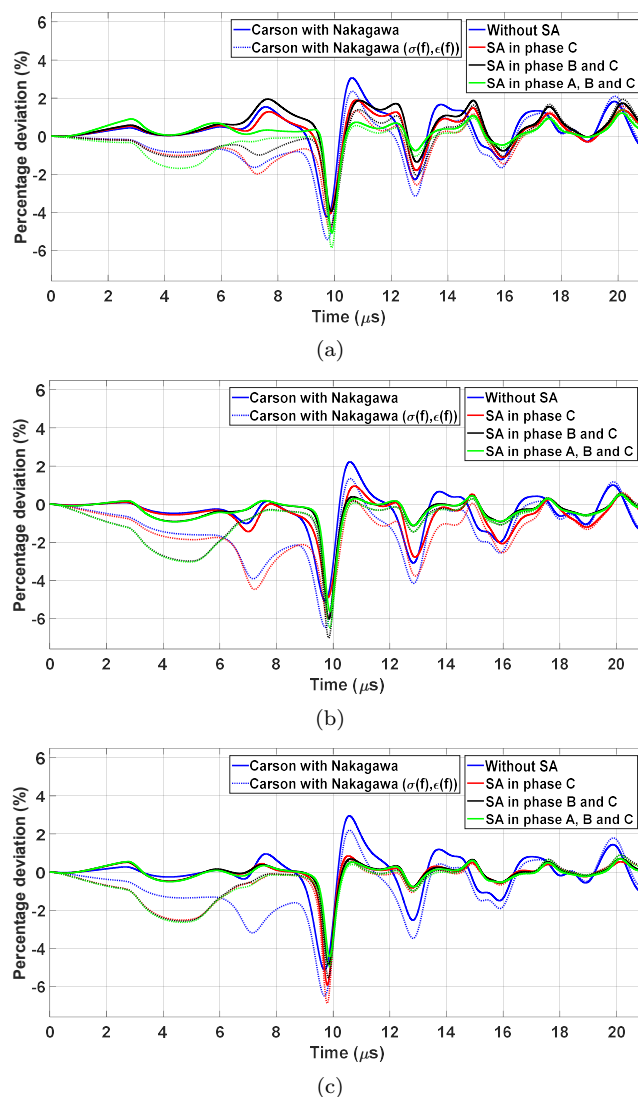


Figure 8. Percentage deviation of the Nakagawa formulation in relations with Carson formulation, considering soil with  $\rho_0=10000 \Omega.m$  in the Fig. 5; (a) Phase A, (b) Phase B and (c) Phase C.

energy dissipated by the device. This last aspect is evaluated in Part II of this paper (Colqui et al., 2022).

## REFERENCES

- Alipio, R., Duarte, M.H., and Lima, A.C. (2018). Influence of grounding representation on the lightning performance of line surge arresters-Part I: Impact on the developed overvoltages. *SBSE 2018 - 7th Brazilian Electrical Systems Symposium*, 1–6.
- Alípio, R.S., De Conti, A., Miranda, A., and Correia De Barros, M.T. (2019). Lightning Overvoltages Including Frequency-Dependent Soil Parameters in the Transmission Line Model. In *Proceedings of the International Conference on Power Systems Transients (IPST)*. Perpignan, France.
- Alípio, R.S. and Visacro, S. (2014). Modeling the frequency dependence of electrical parameters of soil. *IEEE Transactions on Electromagnetic Compatibility*, 56(5), 1163–1171.

- Banjanin, M.S. (2018). Application possibilities of special lightning protection systems of overhead distribution and transmission lines. *International Journal of Electrical Power Energy Systems*, 100, 482–488.
- Carson, J.R. (1926). Wave Propagation in Overhead Wires with Ground Return. *Bell System Technical Journal*, 5(4), 539–554.
- Castro, W.S., Lopes, I.J., Missé, S.L., and Vasconcelos, J.A. (2022). Optimal placement of surge arresters for transmission lines lightning performance improvement. *Electric Power Systems Research*, 202, 107583.
- CIGRE Working Group C4.23 (2021). Procedures for Estimating the Lightning Performance of Transmission Lines – New Aspects.
- CIGRE Working Group C4.33 (2019). Impact of soil-parameter frequency dependence on the response of grounding electrodes and on the lightning performance of electrical systems.
- Colqui, J.S.L., Araújo, A.R.J., Pascoalato, T.F.G., and Kurokawa, S. (2021). Transient analysis of overhead transmission lines based on fitting methods. In *2021 14th IEEE International Conference on Industry Applications (INDUSCON)*, 180–187.
- Colqui, J.S.L., Moura, R.A., Schroeder, M.A.O., and Filho, J.P. (2022). The Impact of Transmission Line Modeling on Lightning Performance of Line Surge Arresters - Part II: Impact on the Power and Energy Dissipation. *XXIV Brazilian Congress of Automatics (CBA)*.
- De Castro, S.A., Do Couto, W.B., Paulino, J.O.S., and Markiewicz, R.L. (2017). Lightning performance of transmission line with and without surge arresters: Comparison between a monte carlo method and field experience. *Electric Power Systems Research*, 149, 169–177.
- De Conti, A. and Emídio, M.P.S. (2016). Extension of a modal-domain transmission line model to include frequency-dependent ground parameters. *Electric Power Systems Research*, 138, 120–130.
- De Conti, A. and Visacro, S. (2007). Analytical representation of single- and double-peaked lightning current waveforms. *IEEE Transactions on Electromagnetic Compatibility*, 49(2), 448–451.
- De Conti, A., Visacro, S., Soares, A., and Schroeder, M.A.O. (2006). Revision, extension, and validation of Jordan's formula to calculate the surge impedance of vertical conductors. *IEEE Transactions on Electromagnetic Compatibility*, 48(3), 530–536.
- Diniz, F.A., Alípio, R.S., and Moura, R.A.R. (2022). Assessment of the Influence of Ground Admittance Correction and Frequency Dependence of Electrical Parameters of Ground of Simulation of Electromagnetic Transients in Overhead Lines. *Journal of Control, Automation and Electrical Systems* 2021, 1–15.
- Gustavsen, B. (2022). URL <https://www.sintef.no/projectweb/vectorfitting/>. Matrix Fitting Toolbox.
- Gustavsen, B. and Semlyen, A. (1999). Rational approximation of frequency domain responses by vector fitting. *IEEE Transactions on Power Delivery*, 14(3), 1052–1061.
- Hileman, A.R. (1999). *Insulation Coordination for Power Systems*. CRC Taylor & Francis.
- IEEE (1992). *Working Group on Surge Arrester*, Modeling of Metal Oxide Surge Arresters. *IEEE Transactions on Power Delivery*, 7(1), 302–309.
- Marti, J.R. (1982). Accurate Modeling of Frequency-Dependent Transmission Lines in Electromagnetic Transient Simulations. *IEEE Power Engineering Review*, 2(1), 29–30.
- Nakagawa, M. (1981). Admittance correction effects of a single overhead line. *IEEE Transactions on Power Apparatus and Systems*, PAS-100(3), 1154–1161.
- Paulino, J.O.S. and Fonseca, B.C. (2019). Effect of high-resistivity ground on the lightning performance of overhead lines. *Electric Power Systems Research*, 172(March), 253–259.
- Prikler, L. and Hoidalén, H. (2009). ATPDraw version 5.6 manual. *European EMTP ATP Users Group*.
- Schroeder, M.A.O., De Barros, M.T.C., Lima, A.C., Afonso, M.M., and Moura, R.A. (2018). Evaluation of the impact of different frequency dependent soil models on lightning overvoltages. *Electric Power Systems Research*, 159, 40–49.
- Vasconcelos, F., Alípio, R., and Moreira, F. (2022). Evaluation of the Lightning Performance of Transmission Lines Partially Protected by Surge Arresters Considering the Frequency-Dependent Behavior of Grounding. *IEEE Latin America Transactions*, 20(2), 352–360.
- Visacro, S. and Soares, A. (2005). HEM: A model for simulation of lightning-related engineering problems. *IEEE Transactions on Power Delivery*, 20(2 I), 1206–1208.
- Visacro, S., Silveira, F.H., Pereira, B., and Gomes, R.M. (2020). Constraints on the use of surge arresters for improving the backflashover rate of transmission lines. *Electric Power Systems Research*, 180, 106064.
- Visacro, S., Soares Jr, A., Schroeder, M.A.O., Cherchiglia, L.C., and de Sousa, V.J. (2004). Statistical analysis of lightning current parameters: Measurements at Morro do Cachimbo Station. *Journal of Geophysical Research*, 109(DO1105), 1–11.